D4.3 Analysis of microclimatic time series and assessment of systematic deviation from local time series required as input in the hygrothermal simulations

Deliverable number	**D4.3**
Deliverable title	**Analysis of microclimatic time series and assessment of systematic deviation from local time series required as input in the hygrothermal simulations**
Nature[1]	**R**
Dissemination Level [2]	**PU**
Author (email) Institution	**Luigi Germinario (luigi.germinario@unipd.it)** **UNIPD**
Editor (email) Institution	**Claudio Mazzoli (claudio.mazzoli@unipd.it)** **UNIPD**
Leading partner	**UNIPD**
Participating partners	**IUAV, OSLOMET, UGR, CVI, VFK**
Official submission date:	**31/08/2021**
Actual submission date:	**07/09/2021**

[1] **R**=Document, report; **DEM**=Demonstrator, pilot, prototype; **DEC**=website, patent fillings, videos, etc.; **OTHER**=other

[2] **PU**=Public, **CO**=Confidential, only for members of the consortium (including the Commission Services), **CI**=Classified, as referred to in Commission Decision 2001/844/EC

Modifications Index	
Date	Version
24/08/2021	0.1 First draft by the Author
31/08/2021	0.2 Second draft with integrations by OSLOMET
31/08/2021	0.3 Final version edited by the WP leader

This work is a part of the HYPERION project. HYPERION has received funding from the European Union's Horizon 2020 research and innovation programme under grant agreement no 821054.

ACRONYMS AND ABBREVIATIONS

µ-XRF	Micro X-Ray Fluorescence
HRAP	Holistic Risk Assessment Platform
HT	Hygrothermal
RH	Relative Humidity
WP	Work Package

Table of Contents

Executive Summary

Deliverable D4.3 presents the work of research and technical development for designing a novel method for monitoring and predicting material decay in cultural heritage. It focuses on the microclimate and climate factors affecting the weathering of stone and timber used as building materials in diverse environmental settings.

An apparatus for long-term field exposure tests was expressly designed in its hardware and software components. That supports the monitoring of the microclimate characteristics of selected stone and wood samples, installed in Italy and Norway at different orientations. The data series of surface temperature and humidity measured on the sample surfaces are to be compared with other microclimate and climate datasets recorded at different scales and from different sources and equipment ("smart tags", weather stations, and regional stations of environmental monitoring). In such a way, the differences between standard climate time series and microclimate series at the scale of both the whole buildings and their discrete component materials can be determined. A correlation is also established between the environmental settings and the material properties and durability. In fact, the apparatus is also designed for the quantification of natural ageing. A series of preliminary laboratory analyses (colorimetry, profilometry, and μ-XRF) were conducted for measuring sample color, surface topography, and chemical composition. The relevant datasets are to be compared with the results of the same analyses repeated in the next years, so to verify changes in material properties and reconstruct the relevant deterioration trends.

The results will feed the HT Simulator Tool and will constantly update the HRAP platform, supporting the modelling of the decay and assessment of the vulnerability of historical building materials, to the benefit of the scholars and stakeholders involved in the protection of cultural heritage from environmental stresses and climate change.

1. Introduction

1.1 Background

The deliverable D4.3 presents a research carried out at UNIPD about the climate and microclimate constraints on the deterioration of building materials used in cultural heritage. This deliverable benefitted from the collaboration and exchange of information with the Hyperion partners IUAV, OSLOMET, CVI, and VFK. It is part of Work Package (WP) 4 and its contents refer to Task 4.2, which is shared with the deliverable D4.5, also edited by UNIPD. The study described here draws on the findings reported in the previous deliverables D4.1 and D4.2, i.e., the petrographic and physical-mechanical characterization of selected building materials of historical significance from Europe and the investigation of their decay. The results will feed the Hygrothermal (HT) Simulator Tool in the framework of the Holistic Risk Assessment Platform (HRAP), modelling the decay and assessing the vulnerability of cultural heritage in diverse climate conditions (Figure 1).

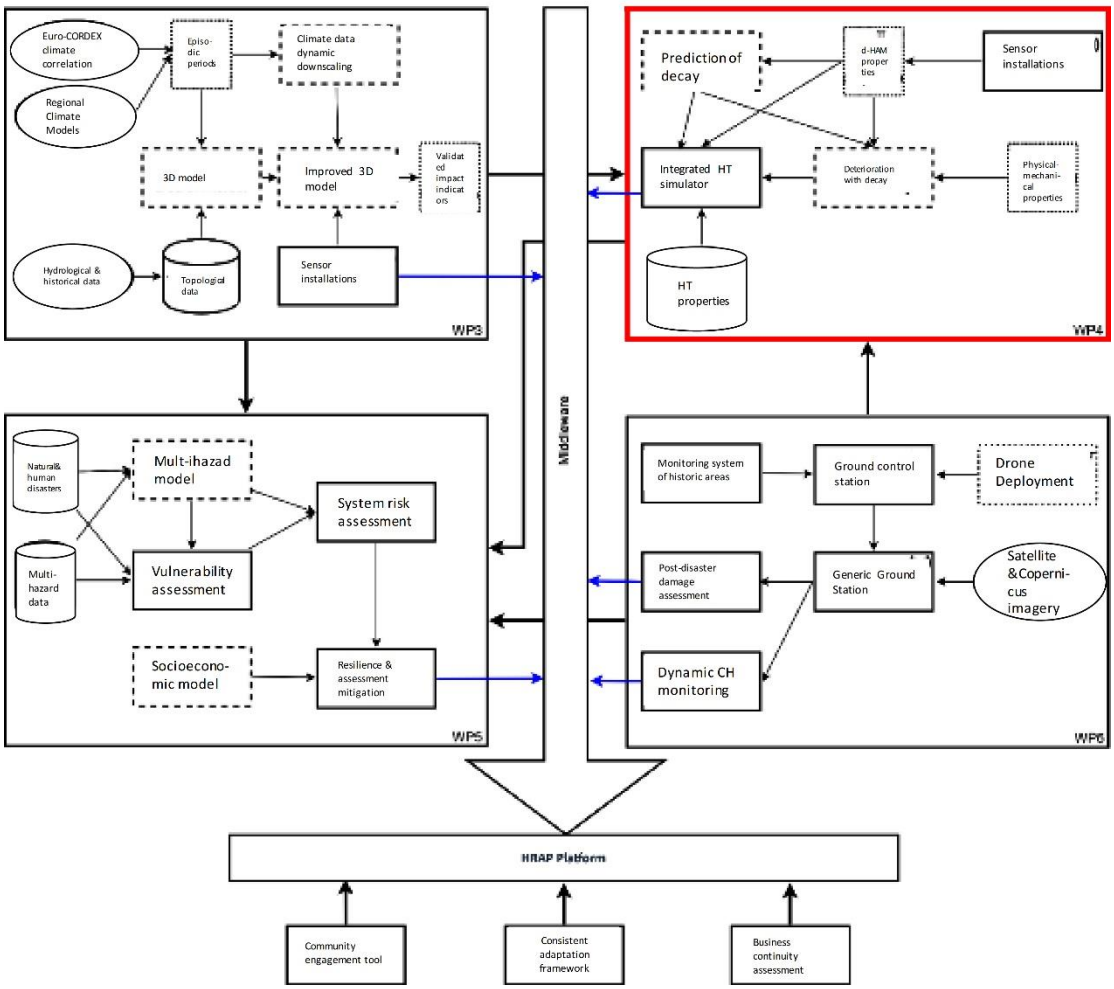

Figure 2: WP4 setting marked in red within the HYPERION's framework, as defined in D2.3.

1.2 Purpose and scope

The research described in D4.3 aims at developing a novel method for the monitoring and long-term prediction of the outdoor weathering of selected building materials (stone and timber), based on critical climate and microclimate parameters and their changes. The direct correlation among different material properties, durability, and environmental settings also provides the preconditions for measuring the differences between standard climate time series and microclimate series at the scale of both the whole building and its discrete component materials. The purpose is to quantify the relevant systematic deviation, which is neglected in most models assessing the climate-related risk to the built heritage. Finally, this deliverable and the findings to be implemented in the next years may provide a reference for all stakeholders involved in the conservation and protection of cultural heritage. In this regard, the final implementation of the HT Simulator is expected to represent a handy tool for assessing climate change risk and the needs for adaptation measures.

1.3 Approach

An apparatus for conducting long-term field exposure tests was designed and built for monitoring the microclimate characteristics and natural ageing and weathering of selected stone and wood samples at different orientations. The equipment was installed (or will be installed in the next weeks) in different locations in Italy and Norway, chosen among the Hyperion partners.

The apparatus will continuously record time series of a set of microclimate parameters measured on all the sample surfaces. The relevant data will be compared with those measured at selected historical sites (including the Hyperion's Tier buildings) by the "smart tags" developed within the project (WP3, D3.4), and the official climate data records published by national or regional agencies. Moreover, the samples will be periodically analyzed (after 12, 24, etc. months) for quantifying the changes in color, surface recession, topography, and chemical composition, comparing the results with those obtained before the equipment installation.

This deliverable sets the time zero for the monitoring activities described above, presenting the design and implementation of the apparatus, the theoretical and practical bases of the study, and the preliminary laboratory analyses. The research will continue in the next years and the updated results will be regularly added to the HRAP.

2. Apparatus

2.1 Hardware design

The hardware for the field exposure tests was conceived and designed specifically for achieving the research goals presented above. It is the result of a careful selection or

original development of the single components, their assemblage, and testing. The equipment was eventually built in three units (for three different locations of installation), named “Cubes” from now on, after their shape. Each Cube has three main components: a stand, a bundle of microclimate sensors, and a control unit.

The stand is an original design, is made of white PVC panels reinforced with a stainless steel frame underneath and has a cubic shape. Two of the stands have each side 100 cm long, the third has each size 50 cm long instead – these dimensions were chosen based on the requirements for the final installation. AISI-304 stainless steel L-hooks were used for fixing the samples to the panels (Figure 2).

The microclimate sensors are two types, for determining temperature and humidity of the sample surfaces. The two sensors are fastened to each sample by using UV-resistant nylon-66 cable ties. The first sensor is the Texas Instruments LM60B, an analog bipolar temperature sensor operating in a range from –25 °C to 125 °C, with an accuracy of ±2 °C at room temperature and ±3 °C over the full range; its output voltage is linearly proportional to temperature (6.25 mV/°C), with a DC offset and a nonlinearity of ±0.6 °C. The second sensor is the Samyoung SY-DS-1, an analog resistive dew sensor operating in a relative humidity (RH) range from 0% to 100% and in a temperature range from 0 °C to 60 °C; it is a switch-type device whose electrical resistance increases sharply in wet conditions, with maxima of 10 kΩ, 100 kΩ, and 200 kΩ at a RH of 80%, 93%, and 98%, respectively (Figure 3).

Finally, the control unit allows for acquiring and storing the microclimate data from the sensors. The electronics have the following three main components: a mux/demux system, an analog-to-digital converter, and a single-board computer (Figure 4).

Figure 2: The 100-cm stand of one of the Cubes with the L-hooks and the control unit box.

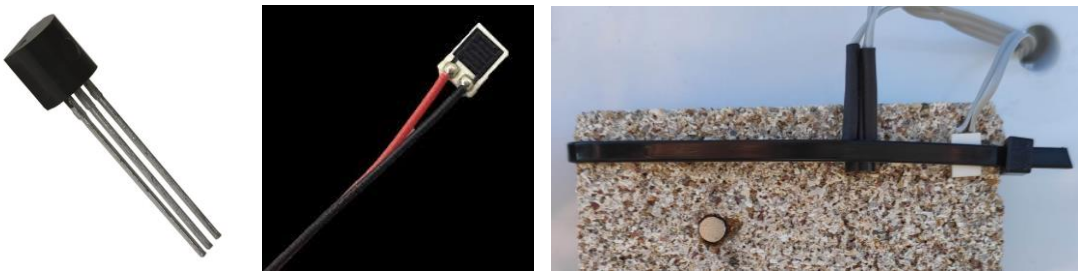

Figure 3: The temperature and humidity sensors and their mounting on one of the stone samples.

Figure 4: The control unit box and the main component boards.

The mux/demux system selects and controls the analog signals of the sensors. It is an original design, and includes a series of boards each including a multiplexer with a complementary demultiplexer, connected with the sensors by ribbon cables; one board controls 16 channels, so that the small Cube has a total of 80 channels (with 5 boards), while the large Cubes have 128 channels (with 8 boards); each channel corresponds to a single temperature or humidity sensor. The system is managed by an additional controller board.

The second component in the chain is a Waveshare High-precision AD/DA board, which converts the analog signal from the sensors and the mux/demux system into a digital signal.

Finally, the converter is connected by a 40-pin GPIO (General Purpose Input Output) to a Raspberry Pi 3 Model B, a single-board computer that processes, writes, and stores the received digital signal. The Raspberry uses a 64-bit Broadcom BCM2837B0 Armv7 processor, a Linux Debian Buster operating system with Raspberry Pi Desktop, a 1-gb RAM, and a 8-gb microSD memory card. The data are continuously saved on the microSD card, periodically uploaded in the internet, and accessed on line using an Ethernet connection directly to the local network or to a Wi-Fi 4G/LTE router Teltonika RUT240 with a slot for a data SIM card.

2.2 Software design

Similar to what has been reported about the hardware, a thorough research or original development was done also for the software packages to be provided with the apparatus for the field exposure tests. The software part performs the tasks of establishing a connection between the user and the Cubes, controlling and monitoring the acquisition of the microclimate data, and also transferring, aggregating, viewing, converting, and saving them on a PC. The standard method of data acquisition involves the logging of the temperature and humidity data from all the stone and wood samples all day every 30 minutes.

Two software packages are original designs, and were developed for connecting the user PC to the Raspberry of the control unit of the Cubes. They allow the communication via TCP/IP and the control on data acquisition and storage. Both were created using C as computer programming language and, as compilers, GNU C for Linux and Borland C++ 5 for Microsoft Windows (Figure 5, 6, and 7).

The software platform is completed by the freeware software VNC Viewer by RealVNC Ltd, used for the remote access and control of the Raspberry; and WinSCP by Martin Přikryl, for data transfer.

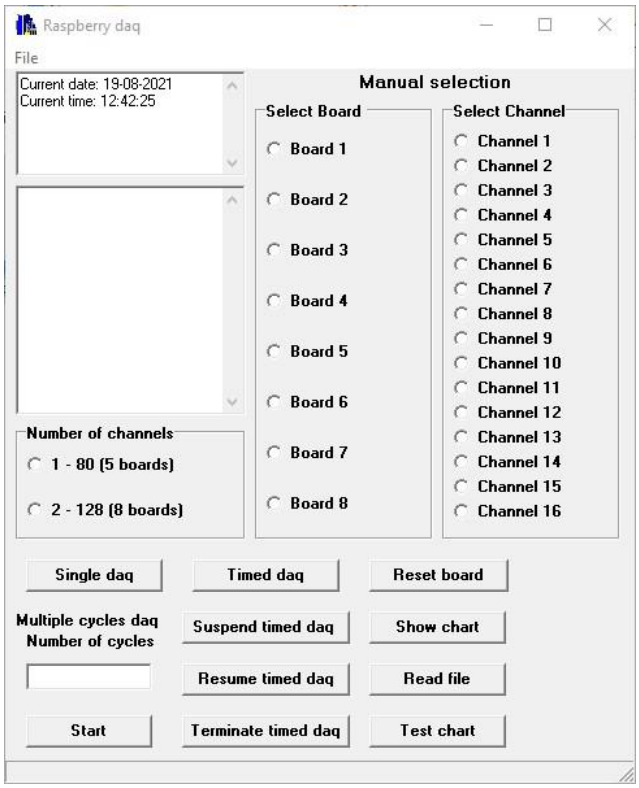

Figure 5: The graphical user interface of the software developed for controlling the acquisition of the microclimate data and testing the sensor operation.

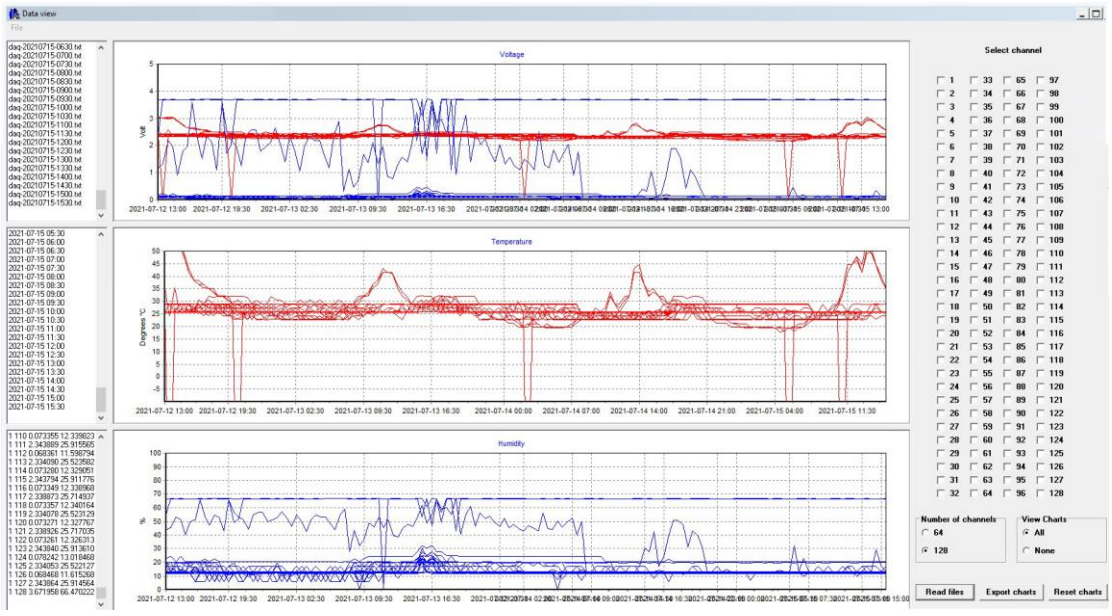

Figure 6: The graphical user interface of the software developed for aggregating, viewing, and exporting the microclimate data.

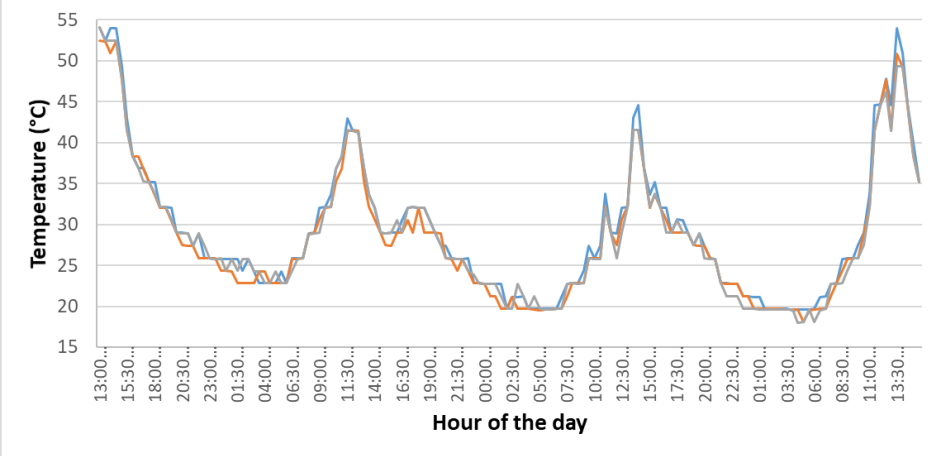

Figure 7: Test monitoring of surface temperature (registered by three sensors) of a stone sample exposed to south in Padua during three days, from 12th to 15th of July, 2021 (only the first and last part of the record refer to sunny hours, while the middle period is associated with cloudy weather).

2.3 Installation

The Cubes were installed (or will be, in the next few weeks) in the following three locations:

- Venice, Italy: on the top of the Clock Tower in St. Mark's Square (45°26'05.2"N, 12°20'20.2"E). That is the Tier 1 building of the relevant Hyperion pilot area.
- Padua, Italy: on the top of the Department of Geosciences of the University of Padua (45°24'31.8"N, 11°53'36.4"E).
- Tønsberg, Norway: on the top of Vestfold Og Telemark Fylkeskommune (59°15'55.9"N, 10°24'57.6"E). That is within 1.5 km from the Tier 1 buildings of the relevant Hyperion pilot area.

These choices were done based on the proximity of the Hyperion pilot areas, the environmental differences among the different sites, and also practical reasons (e.g., installation space, exposure, elevation, availability of electricity and internet connection, accessibility for maintenance, inaccessibility to visitors, etc.).

The small Cube was designed for the installation in Venice and for exposing only the stone samples, for a total of 36 specimens. The two large Cubes, instead, were built for Padua and Tønsberg, for exposing the stone and wood samples together, for a total of 48 specimens (see section 4 "Building materials").

Every panel of the Cubes is oriented in a different direction, making possible the investigation of the microclimate variability and its link with the cardinal direction. In this regard, each Cube has one panel with samples facing north, one facing south, and one horizontal connecting panel (Figure 8).

Figure 8: The Cube installed in Padua.

3. Microclimate and climate data series

3.1 Data sources

The temperature and humidity data series acquired by the Cubes are to be processed and compared with a set of other microclimate and climate data acquired in the same pilot areas but at different scales.

Smart Tags

The measures taken by the Smart Tags provided by the Hyperion partners (WP3, D3.4) will represent the first-order connection between the microclimate characteristics of the single building materials (i.e., the stone and wood samples) and large-scale climate data. In fact, they will give information on the microclimate at the scale of the walls of

the Tier 1 buildings in the Hyperion pilot areas. The Smart Tags are small-size wireless sensor-based network devices that can measure air temperature and RH; moreover, they can calculate the dew point temperature and monitor dry-wet cycles (Figure 9).

At the Tier 1 site in Venice, five smart tags will be installed on the outer walls of the Clock Tower, and one indoors. At the Tier 1 sites in Tønsberg, instead, twelve smart tags in total will be installed, at four different buildings: Bentegården, Fadum storehouse, Heierstad loft (two outdoors and one indoors for each), and the ruins of the Western Tower (three outdoors).

Weather stations

Complementary microclimate time series recorded at the study sites are to be provided by weather stations purposely installed, one in close proximity to each Cube. The weather stations for Venice and Tønsberg were provided by the Hyperion partners (brand Agenso) (Figure 9). The station for Padua, instead, was purchased to the purpose (brand Davis Vantage Pro2). All the stations are to provide time series of air temperature, RH, precipitation amount, wind speed and direction.

Figure 9: The Smart Tag and the weather station provided by the Hyperion partners.

Agencies of environmental monitoring

The last source of climate time series to be consulted are the records published by official agencies of environmental monitoring. They will give a perspective on the regional climate characteristics and topoclimate of the study sites and valid elements for comparing the different environments under investigation.

For Venice and Padua, the source is ARPAV (Regional Agency for the Environmental Prevention and Protection of Veneto). ARPAV provides a set of microclimate

parameters including air temperature, RH, precipitation, wind speed and direction, and solar irradiance. There is one weather station recording these data both in Venice and in Padua (Table 1). Moreover, ARPAV publishes air quality data on the concentration of air pollutants, including CO, NO_x, SO_2, O_3, and PM_{10}; the relevant monitoring stations are differentiated, based on their location in the city, in three types, namely urban traffic, industrial, and background; Venice has two stations in the territory of the historical district (seven, considering the whole municipality), Padua has three (ARPAV 2021). The necessity to monitor the environmental differences between the two cities – even though just 35 km apart – and their impact on cultural heritage conservation have been already highlighted in previous studies; those differences are linked to the proximity to the sea, the diverse industrial concentration, emissions from transports, etc. (Germinario et al. 2017).

For Tønsberg, the source of climate data is the Norsk Klimaservicesenter (Norwegian Center for Climate Services). The center provides time series of air temperature, RH, precipitation, wind speed and direction, and solar irradiance. There are eight weather stations in the city territory logging temperature and precipitation data, whereas the other parameters can be retrieved from the records of nearby stations, e.g., those in Melsom and Ramnes (Norsk Klimaservicesenter 2021) (Table 1).

Table 1: Illustrative climate parameters (T = Mean temperature, Prec. = Total precipitations) in the Hyperion pilot cities recorded in 2020 (sources: ARPAV and Norsk Klimaservicesenter)

	Venice		Padua		Tønsberg	
	T (°C)	Prec. (mm)	T (°C)	Prec. (mm)	T (°C)	Prec. (mm)
Jan	5.7	13.6	4.0	16.8	4.4	99.7
Feb	8.7	5.2	7.9	8.0	2.9	106.8
Mar	10.0	57.2	9.5	59.2	3.7	97.2
Apr	14.6	18.0	14.5	16.8	7.5	29.7
May	18.5	40.6	18.3	36.6	10.6	56.4
Jun	21.6	120.8	21.5	81.8	18.5	99.1
Jul	24.6	29.2	24.4	40.8	15.7	132.1
Aug	25.4	88.2	24.5	123	17.2	77.1
Sep	21.3	129.6	20.5	29.8	13.3	105.1
Oct	14.4	102.0	13.6	99.8	8.4	185.5
Nov	10.1	11.0	8.2	12.4	6.3	122.2
Dec	6.8	96.2	5.9	94.8	3.1	340.9

3.2 Preliminary results

As contingency plan for coping with the delays in the delivery of the equipment described above, a preliminary study was conducted in Tønsberg at selected Tier 1 buildings, for starting the acquisition of microclimate data with complementary sensors. The sensors measure air temperature and RH every five minutes. They were installed in the Fadum storehouse and the Heierstad loft, as shown in Figure 10. Specifically, sensors A and C were placed in the interior of the Fadum storehouse, while sensors B and D were installed on the exterior of the north- and south-oriented walls, respectively; they are shielded by the shed surrounding the building. As for the Heierstad loft, sensors F and H were placed in the interior, while sensors E and G were mounted on the exterior of the northeast and southwest walls, respectively.

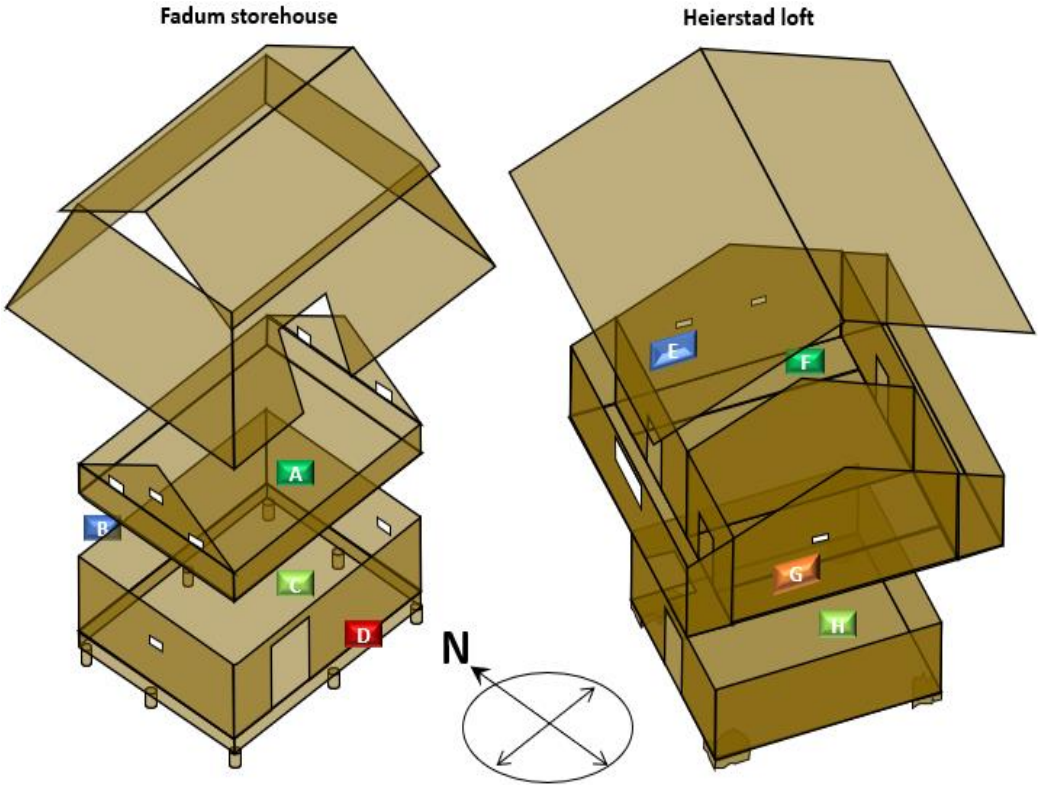

Figure 10: Positions of the air temperature and RH sensors in the Tier 1 buildings in Tønsberg.

Figure 11 presents the air temperature and RH measures, referring to the period from 7 May 2021 until 10 August 2021. There are significant differences among the different exposure environments, i.e., among different orientations as well as between indoors and outdoors. The most significant are observed between the northern and southern surfaces. The differently oriented sides also show the most significant differences in terms of deterioration patterns (Choidis et al. 2021). The south-oriented surfaces are more exposed to solar radiation and driving rain, and record higher temperature and lower RH levels; they are also associated with the most intense weathering in terms

of discoloring, checks, and splits (Figures 12 and 13). On the other hand, the north-oriented surfaces are less exposed to solar radiation and remain wet longer, so their temperature is the lowest, while RH is the highest; these microclimate conditions favor the growth of biological organisms, such as algae, fungi, and lichens (Figures 12 and 13).

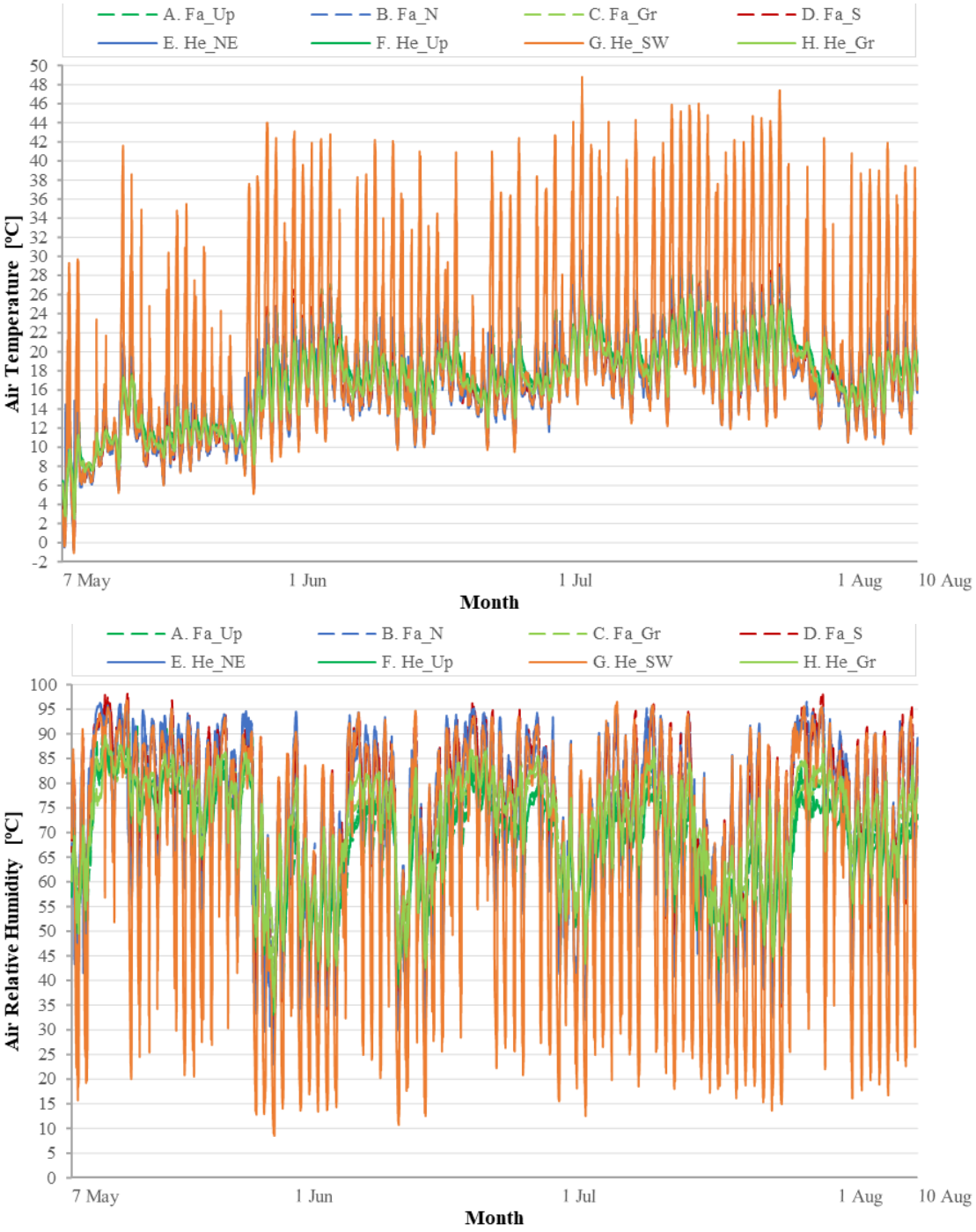

Figure 11: Air temperature and RH in the Fadum storehouse and Heierstad loft (7 May to 10 August 2021).

Figure 12: At the Fadum storehouse, the growth of biological organisms is more intense on the north façade (left) than on the south façade (right) (Choidis et al. 2021).

Figure 13: At the Heierstad loft, the northeast façade is colonized by algae (left), while the southwest façade has several checks, splits, and discoloring due to weathering.

4. Building materials

4.1 Selection and preparation

The stone and wood samples installed in the Cubes were prepared selecting a number of building materials based on two main criteria: their importance and usage in cultural heritage in Europe in different environments and, specifically, in the Hyperion's Tier buildings; their properties, covering a range of diverse compositional and textural characteristics, so to set a reference for other similar historical building materials. Extensive information on their properties and durability can be found in D4.1 and D4.2, also edited within WP4.

Stone

The selected stone materials come from different quarries located in Italy, Greece, Spain, Norway, and Croatia (Table 2, Figure 14). With regard to their usage in the Tier buildings, Carrara marble, Red Verona, and Istria stone are all observable in the wall claddings of the Clock Tower of Venice. In Tønsberg, instead, the stones used are

Tønsberg latite and Tønsbergite (e.g., in the Western Tower and in the foundations of the Bentegården).

Table 2: List of the stones investigated.

Country	Stone name	Supply	Rock type	ID
Italy	Botticino	Nordexplo' SRL	Limestone (sedimentary)	BL
	Carrara marble	Nordexplo' SRL	Marble (metamorphic)	CM
	Costozza stone	Nordexplo' SRL	Limestone (sedimentary)	CS
	Euganean trachyte	Nordexplo' SRL	Trachyte (volcanic)	ETR
	Red Verona	Nordexplo' SRL	Limestone (sedimentary)	RV
Greece	Lartios stone	Petrodiaskosmitiky Kyriazis Bross	Sandstone (sedimentary)	LS
	Sfouggaria	Petrodiaskosmitiky Kyriazis Bross	Limestone (sedimentary)	SS
Spain	Macael marble	Tesela	Marble (metamorphic)	MM
	Santa Pudia	Tesela	Limestone (sedimentary)	GSP
Norway	Tønsberg latite	Oslo University	Latite (volcanic)	TRH
	Tønsbergite	Oslo University	Monzonite (intrusive)	TSY
Croatia	Istria stone	Nordexplo' SRL	Limestone (sedimentary)	IS

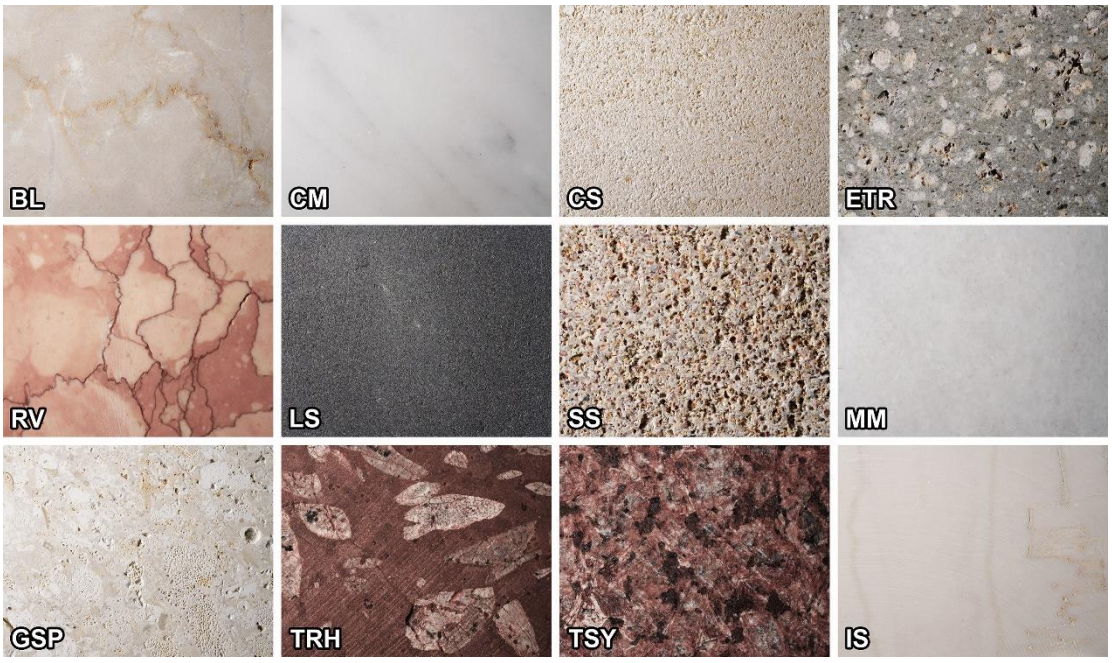

Figure 14: Photos of the stones marked by their IDs (short side = 4 cm).

All the samples were cut into 70x70x20 mm tiles. Secondly, they were drilled through and an AISI-304 stainless steel cylinder was inserted in each specimen and glued with a two-component epoxy resin Kömmerling Körapox 439. Finally, the surface of the whole tile was levelled and roughly polished with 60-grit sandpaper. A total of 108 specimens were selected for the field exposure tests and the preliminary laboratory analyses; that is, one specimen for each stone variety to be installed on each panel (facing north, south, and horizontal) of each of the three Cubes, or 12 specimens in total for each panel.

Wood

The selected wood materials come from the forest area of Vikersund, Modum Municipality, in Norway, and include different types of pine and spruce (Table 3, Figure 15). Timber of the same species is used in the Tier buildings of Tønsberg, i.e., in the Bentegården, Fadum storehouse, and Heierstad loft.

Table 3: List of the wood materials investigated.

Genus	Type	ID	Supply
Pine	Densely grown with high amount of core wood (up to 100%)	F1	Kjølstad sawmill
Pine	Fast grown with minor or no core wood	F2	Kjølstad sawmill
Spruce	Densely grown	G1	Kjølstad sawmill
Spruce	Fast grown	G2	Kjølstad sawmill

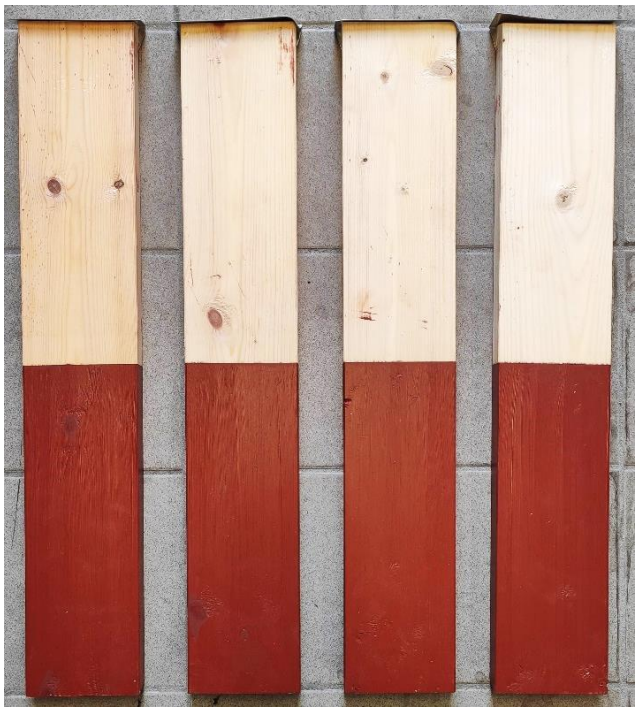

Figure 15: Photos of the wood samples with the metal flashing on the top.

The timber supplied was cut into 600x102x23 mm samples, hand-levelled on three sides, and air-dried reaching a moisture of 10-13%. The upper half of each specimen was left without finish. The lower half, instead, was treated on the surface with a red paint made from pure linseed oil (by Ottosson Färgmakeri AB, Sweden), applied in three layers; the red color is given by iron and zinc oxides. Finally, a zinc flashing was mounted on the top of the samples of the vertical panels of the Cubes, to prevent water penetration into the end grain. A total of 24 specimens were selected, that is, one specimen for each wood type to be installed on each panel (north, south, and horizontal) of each of the two large Cubes, or 4 specimens in total for each panel.

4.2 Baseline analyses

Before the final installation in the Cubes, the stone samples were investigated in the laboratory in order to set a time-zero baseline, which would serve as reference for the same analyses to be repeated after 12, 24, etc. months of exposure. All the 108 samples were photographed and analyzed by colorimetry and profilometry. Moreover, a subset of 24 samples were also analyzed by micro X-ray fluorescence (μ-XRF). The stone properties to be monitored are color, surface topography (and recession), and chemical composition.

Colorimetry

A portable spectrophotometer 3nh NS800 was used for the colorimetric analyses, following the recommendations of the standard EN 15886 (2010). The measures were done in the CIELAB color space, thus defining the color with the three coordinates of lightness (L*), red/green proportion (a*), and yellow/blue proportion (b*). A CIE standard illuminant D65 was used, with the CIE standard observer at an angle of 10°. The total color differences are to be calculated with the CIEDE2000 formula (ΔE^*_{00}). 10 measures per sample were taken, that is, a total of 1,080 measurements. For the future analyses, the measure reproducibility is assured by the use of a rigid mask applied to the samples during the operations.

Table 4 collects basic statistics of the colorimetric dataset. The materials showing the highest standard deviations are the stones with visible and frequent stylolites, or diversely colored matrixes, or with coarse grain size (e.g., with phenocrysts).

Profilometry

The 3D surface topography of the stone samples was analysed with a portable 3D non-contact optical profilometer Nanovea JR25, equipped with an optical pen providing a vertical resolution of 17 nm within a measurement range of 1.1 mm. The following analytical conditions were applied: 20x10 mm scanned area, 10 μm step size, 400 Hz acquisition rate, and averaging of 2 measures per spot. Every scan started from a slice of the stainless steel cylinder mounted in each sample, which will represent a reference for the future repeated analyses aimed at quantifying stone recession compared to a corrosion-resistant material.

Table 4: Summary of the colorimetric measures for all the stones analyzed.

	L*	a*	b*	L*	a*	b*
	Average			Standard deviation		
BL	77.01	1.34	9.19	1.86	0.51	1.28
CM	85.86	-0.98	0.08	1.04	0.10	0.68
CS	88.34	1.49	11.24	0.61	0.17	0.78
ETR	63.16	-0.17	6.21	2.70	0.29	0.74
GSP	90.78	0.35	8.32	1.12	0.13	1.24
IS	78.14	0.57	7.89	1.05	0.20	0.92
LS	44.40	-0.70	-0.07	1.37	0.12	0.67
MM	76.86	-1.32	-1.38	2.90	0.11	0.45
RV	63.97	11.72	16.07	2.74	1.77	2.61
SS	68.25	2.94	11.49	1.43	0.31	0.79
TRH	41.91	5.21	6.09	3.57	0.84	1.00
TSY	47.65	5.37	5.04	4.67	0.95	0.83

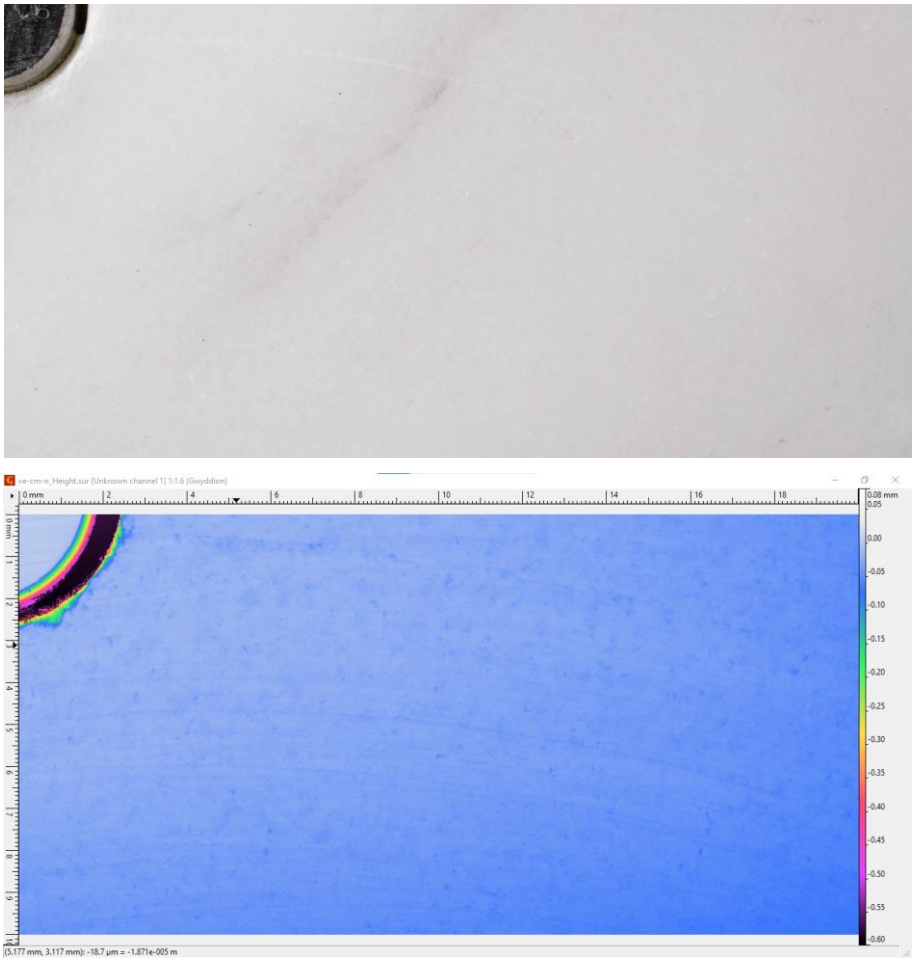

Figure 16: Macro photo and corresponding profilometric map of a sample of Carrara marble (CM). The top left corner is taken up by the reference stainless steel surface.

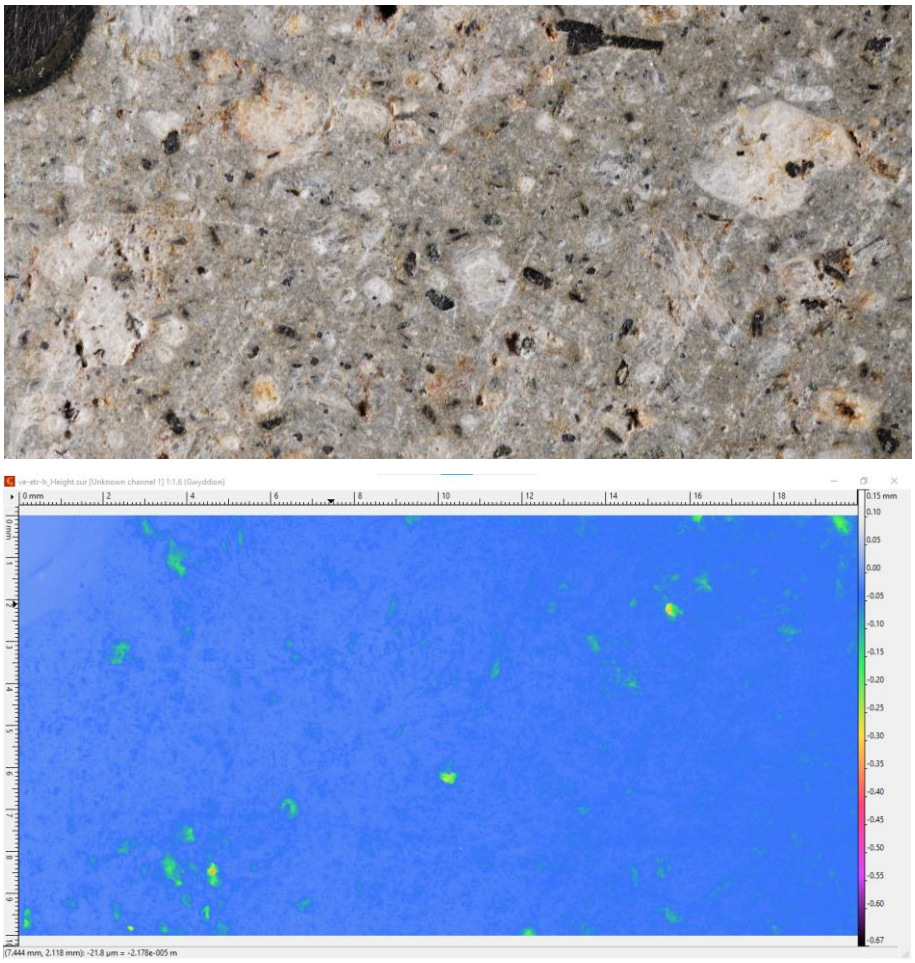

Figure 17: Macro photo and corresponding profilometric map of a sample of Euganean trachyte (ETR).

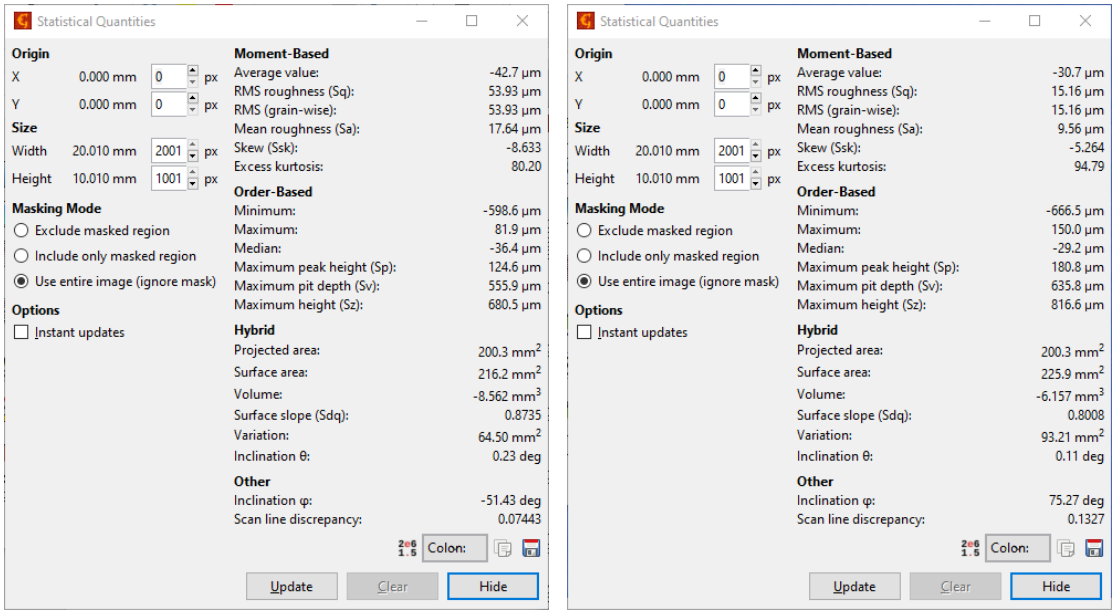

Figure 18: Example of basic statistics calculated on the maps of samples CM (left) and ETR (right).

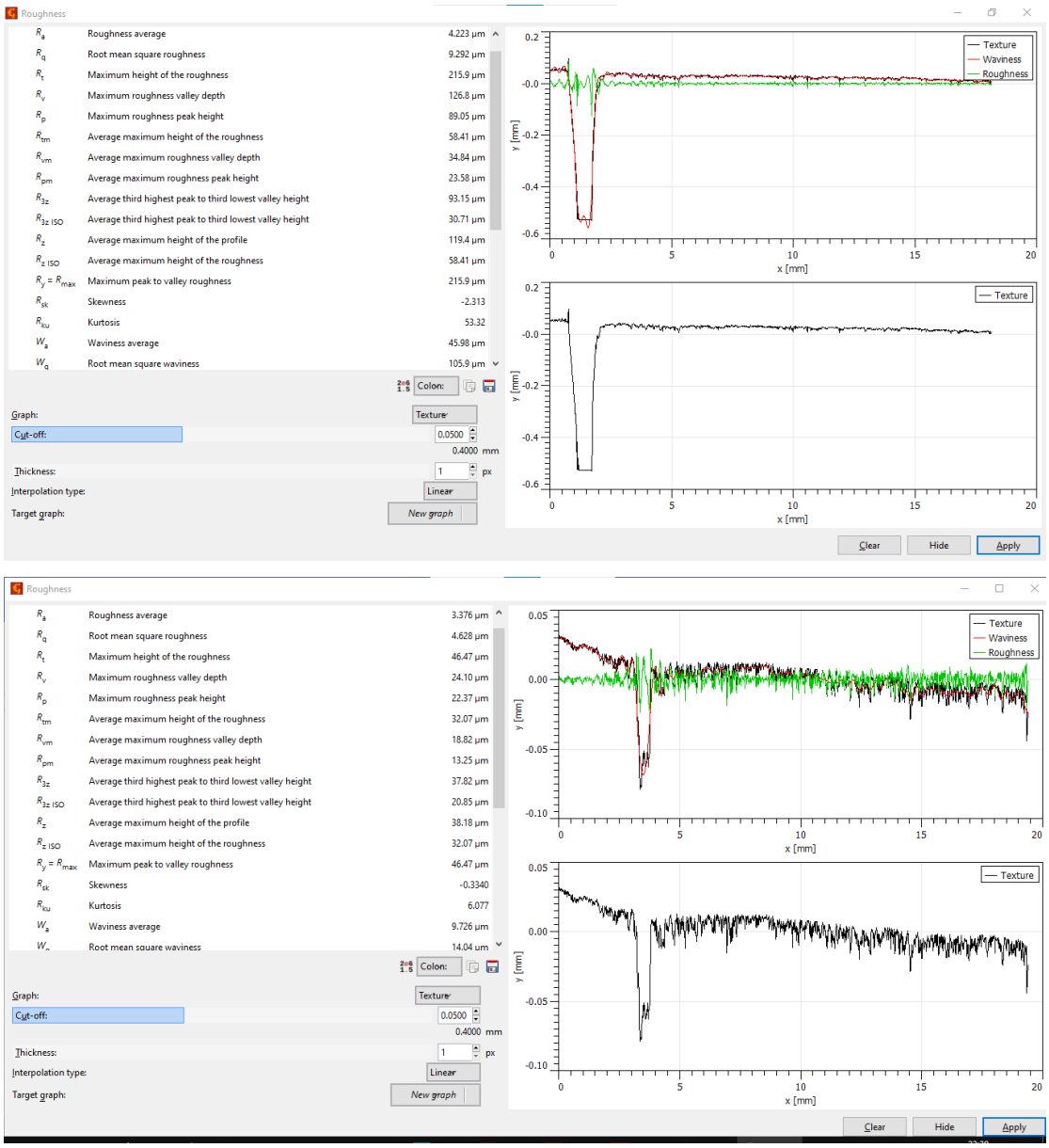

Figure 19: Statistical analysis of profiles traced on the maps of samples CM (top) and ETR (bottom), starting from the reference stainless steel surface (left) and continuing on the stone.

Apart from the surface recession quantification, the profilometry will allow for determining changes in roughness, texture, size and shape parameters, etc. The map processing is done with the freeware software Gwyddion (Department of Nanometrology, Czech Metrology Institute). In Figure 16, 17, 18, and 19 some illustrative results are shown.

µ-XRF

The 2D chemical composition of the stone samples was analyzed by µ-XRF mapping, using a bench-top spectrometer Bruker M4 Tornado (IUAV), equipped with an X-ray tube with Rh anode and a silicon-drift detector with Be window. The following

analytical conditions were applied: 20x20 mm mapped area, 200 spots measured, 20 µm spot size, 200 ms dwell time (500 µm/s rate), with the X-ray tube operated at 50 kV and 200 µA. The following elements were detected: Na, Mg, Al, Si, P, S, Cl, K, Ca, Ti, Mn, Fe, Cu, Zn, As, Pb, Sr, Zr, Ba, Bi, Cd, Co, Cr, Mo, Ni, Sb, Sn, V. Figure 20, 21, and 22 and Table 5 show some illustrative results from representative samples.

Coupling µ-XRF maps with digital image analysis opens a series of possibilities for quantifying the texture, geometrical features of the rock components, and abundance ratios of different phases (Germinario et al. 2016). This follows the detection of chemical alteratio, formation of secondary phases, or deposition of exogenous compounds, revealed by changes in the surface chemistry of the stone tiles outdoors.

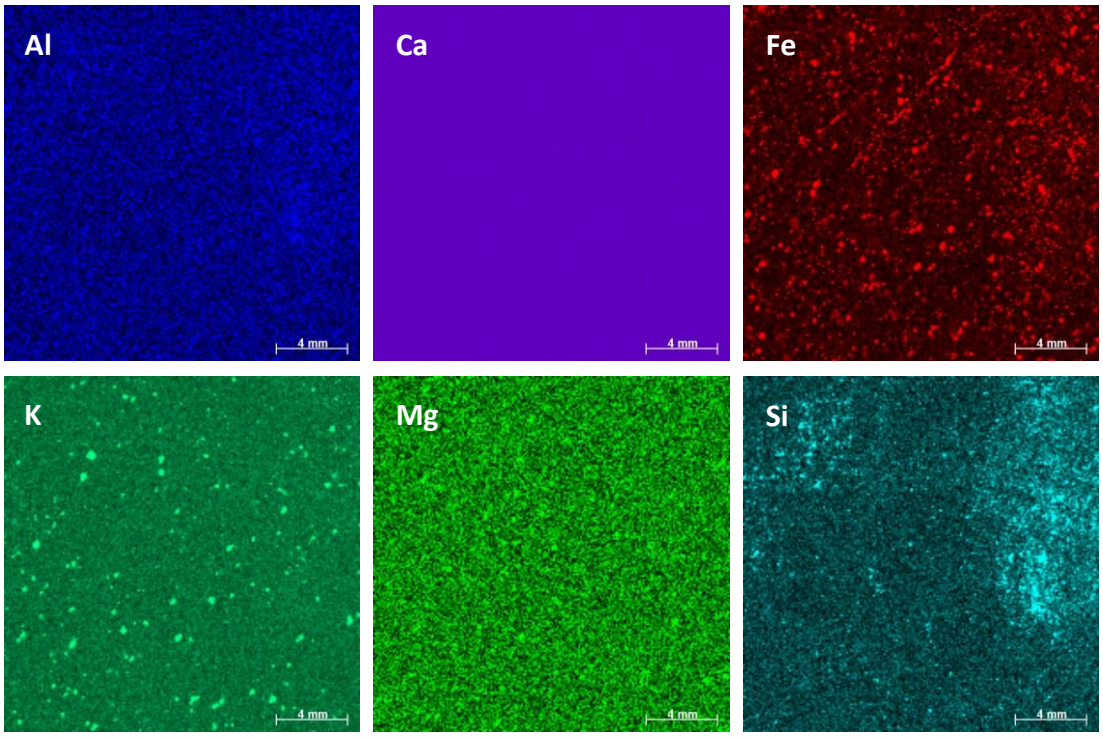

Figure 20: µ-XRF elemental maps obtained on a sample of Carrara marble (CM).

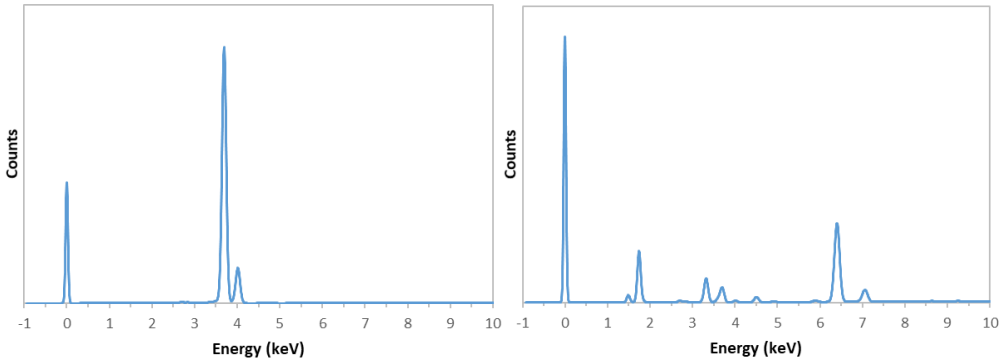

Figure 21: µ-XRF spectra of samples of Carrara marble (CM, left) and Euganean trachyte (ETR, right).

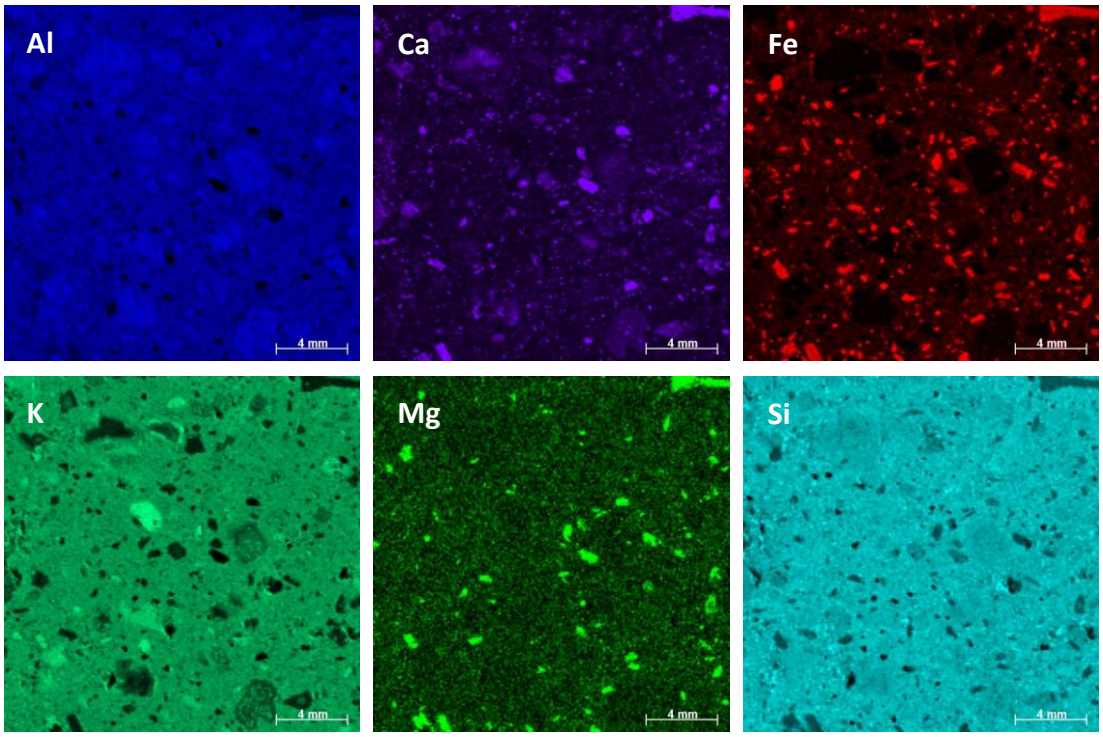

Figure 22: µ-XRF elemental maps obtained on a sample of Euganean trachyte (ETR).

Table 5: Semiquantitative chemical analysis by µ-XRF of samples CM and ETR (elemental concentrations expressed as weight % and normalized weight %).

	CM		ETR	
	wt%	norm. wt%	wt%	norm. wt%
Na	0.17	0.27	3.16	5.64
Mg	0.49	0.78	0.25	0.45
Al	0.18	0.29	8.62	15.38
Si	0.15	0.24	30.95	55.27
P	0.00	0.00	0.03	0.06
K	0.00	0.00	5.81	10.38
Ca	61.89	98.21	2.71	4.84
Ti	0.00	0.01	0.59	1.06
Mn	0.02	0.04	0.09	0.15
Fe	0.02	0.04	3.53	6.31

5. Photogrammetric evolution of deterioration

5.1 Locations with different environmental conditions

In order to quantify the influence of weather on the Santa Pudia Calcarenite (SPC in what follows) three different heritage buildings have been considered. The three SPC historical buildings are located in three different towns of the province of Granada (South of Spain, see Figure 23), characterized by different weather conditions. The location of the monument are indicated with stars in Figure 23.

A brief description of each of them is presented bellow.

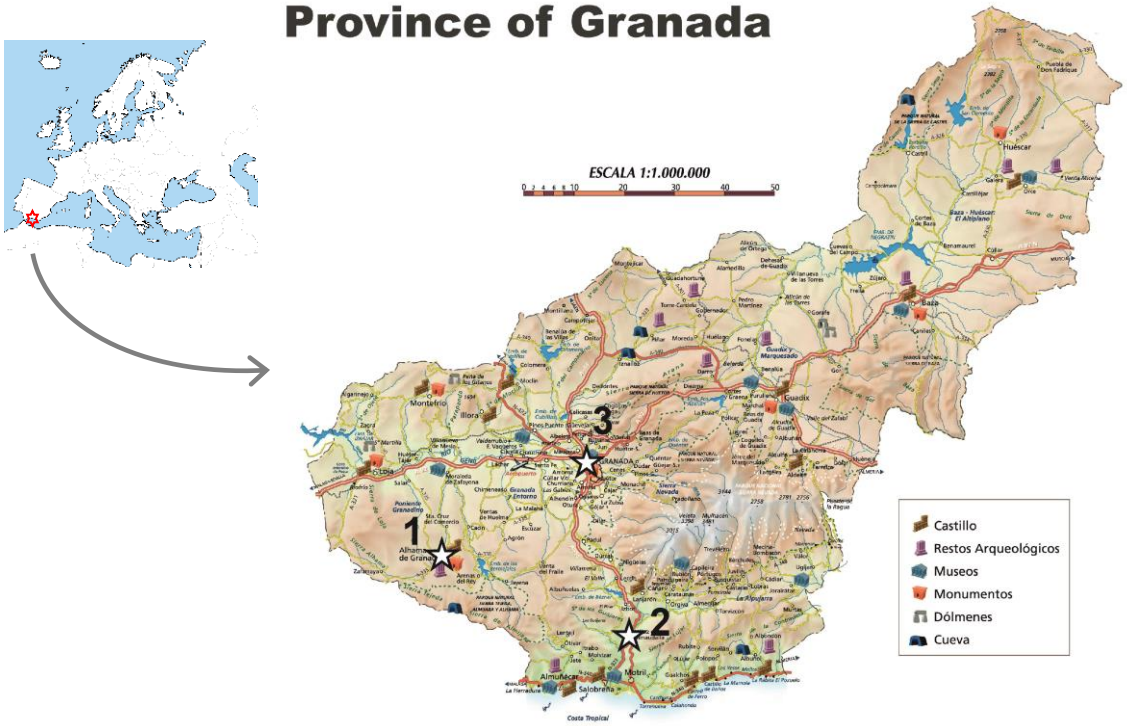

Figure 23. Province of Granada, Spain, with the location of the three considered localities: 1) Alhama de Granada; 2) Vélez de Benaudalla; 3) Granada (adapted from https://ontheworldmap.com/spain/city/granada/province-of-granada-map.jpg).

The Church of Nuestra Señora del Carmen of Alhama de Granada

Alhama de Granada is a town whose geographical coordinates are 37° 0' N, 3° 59' W (Figure 23). It is located at an altitude of 895 meters. Alhama de Granada is known for its Arab thermal baths located on the remains of the Roman baths and from which its own name comes ("al-Hama" means the bath).

The Church of Nuestra Señora del Carmen (Figure 24) was built between 1589 and 1619. Later, in 1634 the sacristy was added. The church, which is made entirely of calcarenite stone from the Santa Pudia quarry, is divided into two modules. As can be

seen in Figure 1, one module is hexagonal in shape and is attached to the main nave of the church.

In the 1884 earthquake the suffered important damage and it was restored. The small tower in the right was built in the 19th century.

Figure 24. The Church of Nuestra Señora del Carmen in Alhama de Granada.

The Church of Nuestra Señora del Rosario of Vélez de Benaudalla

Velez de Benaudalla is located at 36º 50' N and 0º 10' W, at an altitude of 173 meters above the sea level. This town is in the tropical coastal region of Granada and it is surrounded by mountain ranges that reach up to 1500 meters. It is located on a gentle slope.

The current Church of Nuestra Señora del Rosario de Vélez de Benaudalla was built between 1778 and 1784. It was built on the foundations of two previous temples, the first of which was ruined by a fire. The church has a Neoclassical style being the plant of the church a cross that is inscribed within a square. It is made up of three naves.

As can be seen in Figure 25, also this church is made of calcarenite.

Figure 25. The Church of Nuestra Señora del Rosario of Vélez de Benaudalla.

The Church of San Jerónimo monastery of Granada

Granada city is located at 37°11’ N and 3°36’ W, 689 m above sea level. The Church of the Monastery of San Jerónimo was ordered to be built in 1504 in the Gothic style of the period but in 1526 the new architects (Jacobo Florentino and Diego de Siloé, who also was the architect of the Cathedral of Granada) change Gothic architecture by a new Renaissance aesthetic.

The church, which was started to build in 1519, has a Latin cross plan with a polygonal apse. At the foot of the church is the tower, finished in 1565, which was demolished in its upper half at the beginning of the 19th century and rebuilt in the 20th century. As can be seen in Figure 26, one of the lateral facades of the church is attached to a cloister.

The church is also made of Santa Pudia calcarenite (Figure 26).

Figure 26. The Church of San Jerónimo monastery of Granada.

5.2 Photogrammetric study of deterioration

The surface recession of the above three heritage buildings are studied based on digital photogrammetry, a simple non-destructive technique already used for this purpose (Jalón et al., 2021). Two zones affected by degradation of each building have been photographed using a digital still camera (Nikon D7200, 18 mm focal length). The images are then post-processed and a 3D photogrammetric point cloud (PPC) is generated. Finally, the degradation profiles are obtained from the PPC using the open source software CloudCompare (Girardeau-Montaut, 2016).

The photogrammetric data is obtained up to a certain level above the ground level since the upper part of the building does not show visible deterioration. The zero deterioration depth is determined by visual inspection and it is adopted as the reference for the measurements.

Figures 27 to 29 show the degradation profiles of the building studied. In Figures 27 to 29 the mean values adjusted by linear regression (least-square) are represented with a black line. The level of dispersion is quantified through the standard deviation SD and the values of the SD (i.e. mean ± SD) are also indicated in Figures 27 to 29 with dashed lines.

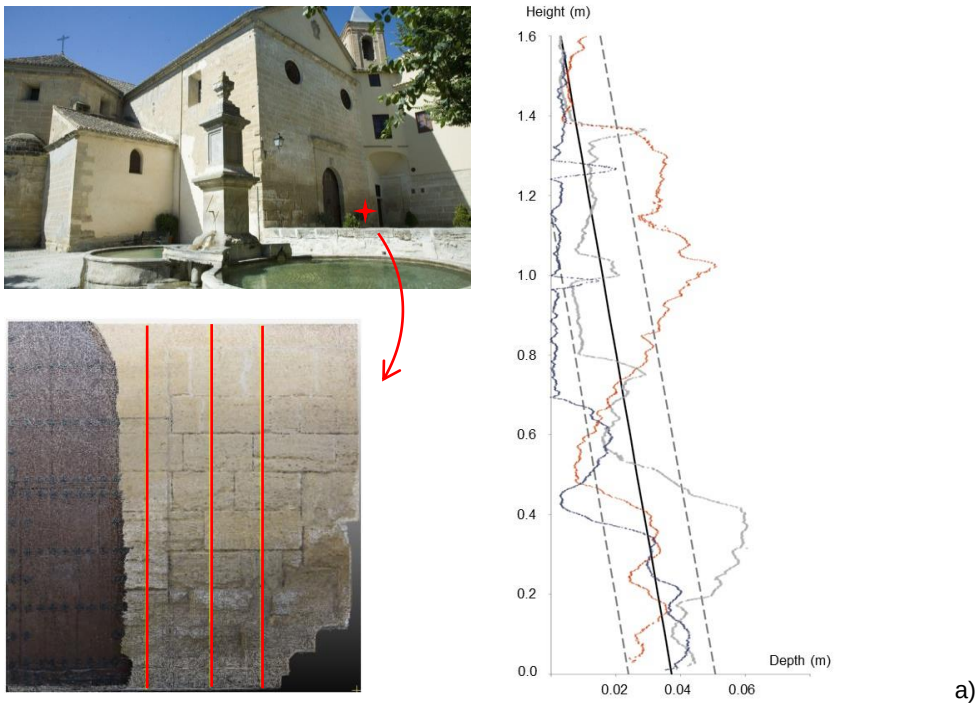

Figure 27. Recession patterns of Alhama de Granada. a) Main façade (NW orientation). b) Lateral façade (NE orientation).

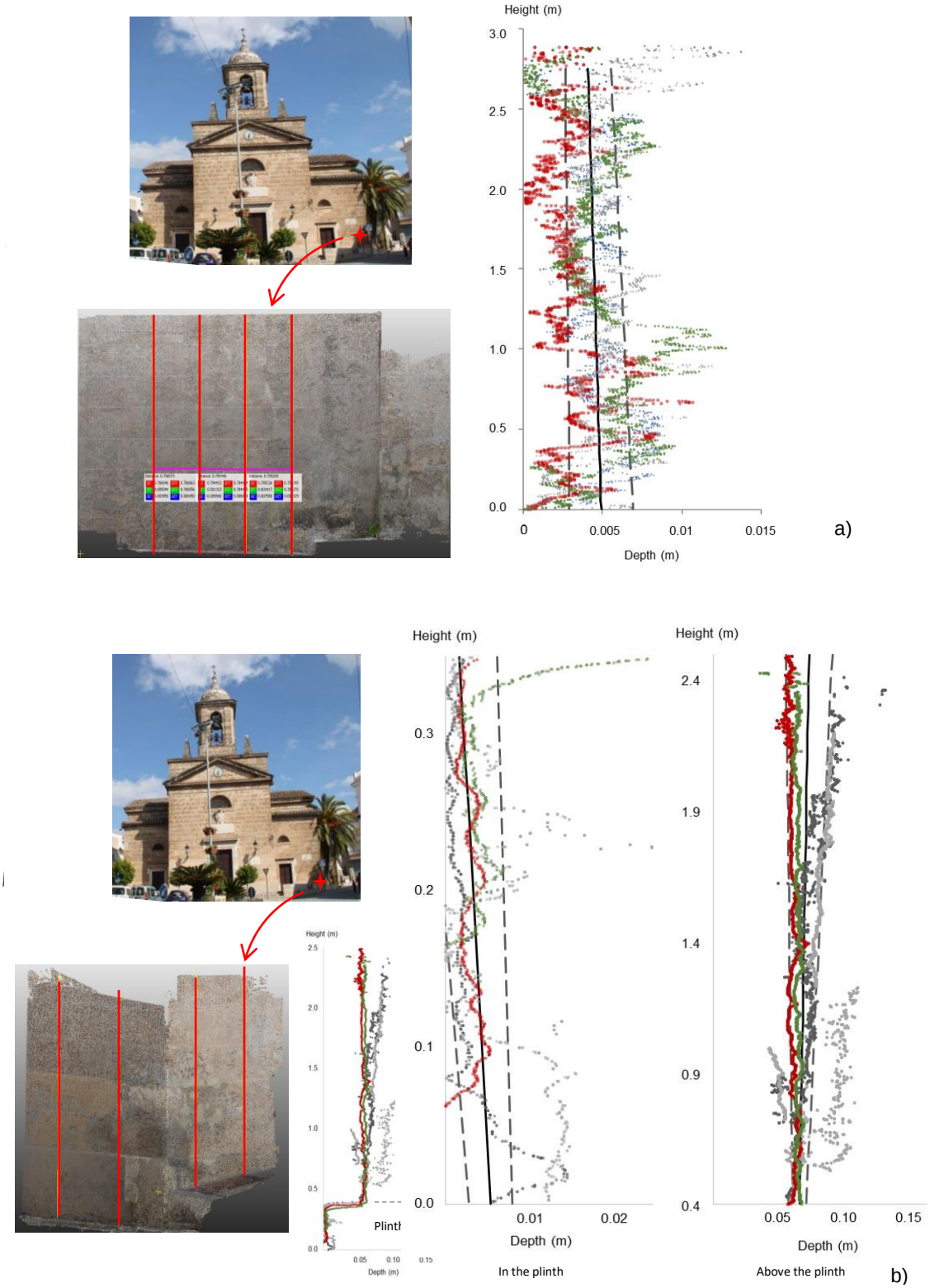

Figure 28. Recession patterns of Vélez de Benaudalla. a) Main façade (SE orientation). b) corner (S orientation).

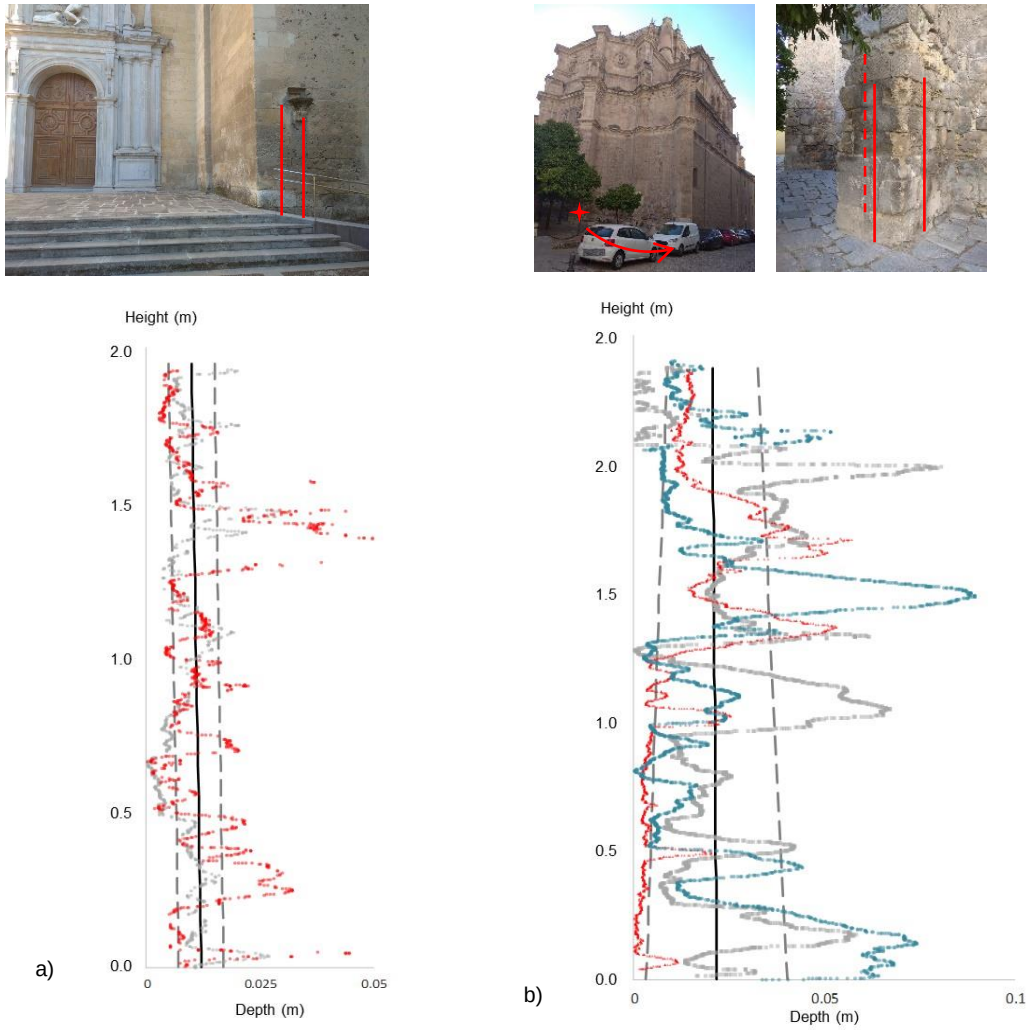

Figure 29. Recession patterns of San Jerónimo. a) Main façade (NW orientation). b) buttress (SE orientation).

In the church in Figure 27 three sections located at the right side of the main entrance door and five sections of the lateral façade are analysed (Figures 27a and 27b, respectively). As can be seen in Figure 27b, in the lateral façade degradation is concentrated below the small stone ledge existing at around 1 m above the ground level. In both façades of the church of Nuestra Señora del Carmen of Alhama de Granada a triangular degradation pattern are obtained (Figure 27).

In the case of the Church of Nuestra Señora del Rosario of Vélez de Benaudalla four section in the middle of the main façade and another four sections around the right corner of the main façade are studied (Figures 28a and 28b). Around the corner there is an around 0.4 m height plinth. In this zone, the adjustment has been divided in two: in the plinth and above it (see Figure 28b). As can be seen in Figure 28, degradation in

the plinth matches a triangular pattern while both around the corner and above the plinth a square pattern is better adjusted.

Regarding the Church of San Jerónimo, two section in the right side of the main façade and three sections in one of the buttress located behind apse are studied. In the case of the buttress one section at each of the three faces of the element are selected (Figure 29b). As can be seen in Figure 29 degradation match square pattern in both cases. It is interesting to remark that very close to the buttresses there is a group of trees (see Figure 29b) which impedes the lower part of the apse is exposed to the sun, which lead to keep moisture in this zone.

The mean area affected by degradation for the cases studied is summarized in Table 6 (see Figures 27 to 29). In this table, the approximate age and the height affected by deterioration have also be summarized.

Table 6. Average area affected by degradation.

Heritage building	Year of construction	Location	Affected height (m)	Average degraded area (m^2)
Church of Nuestra Señora del Carmen of Alhama de Granada	1589	Main façade (NW)	1.60	0.0323
		Lateral façade (NE)	1.00	0.0238
Church of Nuestra Señora del Rosario of Vélez de Benaudalla	1778	Main façade(SE)	2.75	0.0123
		Corner (S)	2.50	0.0080
Church of San Jerónimo monastery of Granada	1519	Main façade (NW)	2.00	0.0213
		buttres (SE)	2.37	0.0500

5.3 Environmental conditions

A study of the more relevant climatic factors influencing the deterioration of SPC is carried out. Given the particularities of SPC already commented, this study is focused on two measurements: the number of days with temperatures below zero and precipitations (mm).

In Figures 30a and 30b the available records obtained from the official web site [AEet, Junta de Andalucía] are represented. Figure 30a shows the number of days with temperatures below zero per year along the historical series while Figure 30b summarizes the total annual precipitation. Table 7 summarizes the average value of this measured for the three locations studied.

a)

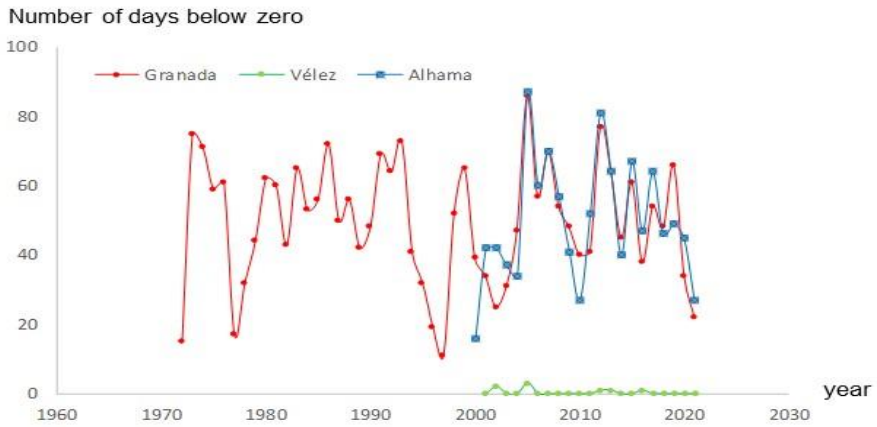

b)

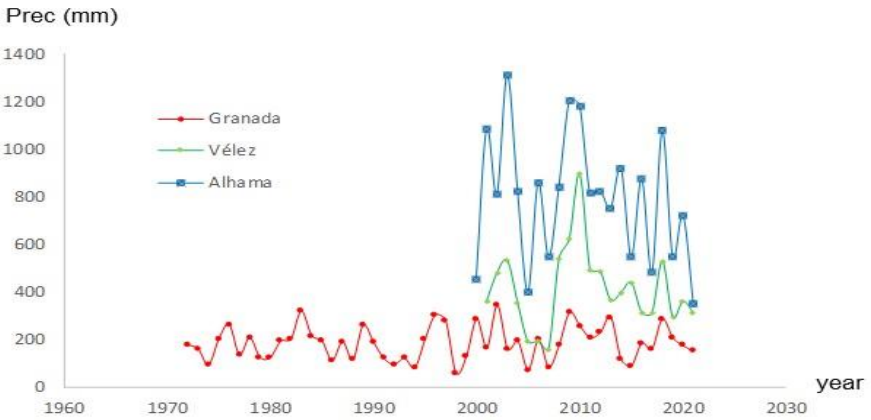

Figure 30. Available records of the number of days per year with temperature below zero (a) and of annual precipitation (b) obtained from the official web site [AEet, Junta de Andalucía].

Table 7. Average climatic factors considered.

Location	Annual number of days with temperature below zero	Annual precipitation (mm)
Alhama de Granada	49.77	791.08
Vélez de Benaudalla	0.38	409.36
Granada	49.76	183.46

6. Conclusions

This deliverable presents the work of research and technical development for designing a novel method for monitoring decay processes in cultural heritage. It helps assessing the interaction of the building materials with the environment and their weathering constrained by microclimate and climate variability and the stresses brought about by climate change.

From this perspective, the study described in D4.3 is at the forefront of the risk assessment of heritage materials and assets. In fact, it lays the foundations of a long-term investigation of the natural behavior of building materials in different natural environments, constantly updated in the framework of the HRAP as the materials deteriorate and the environmental setting changes. The findings might represent a source of precious information for the activities and decision-making protocols of the stakeholders involved in the protection of cultural heritage.

This approach marks a step forward in respect to the traditional laboratory studies of materials subjected to artificial accelerated ageing tests – which often do not find direct and straightforward correlations with natural ageing; and to other recent works dealing with field exposure tests. D4.3 clarifies the importance of considering the microclimate measured at the material surface, the correlation and possible deviations from standard climate time series, the impact of different orientations, and a range as wide as possible of different materials and environmental settings to be examined. These aspects are tackled very rarely in the literature, even more so if considered all together (Ghedini et al. 2011; Roots et al. 2011; Daly 2014; Haugen et al. 2018).

7. REFERENCES

1. ARPAV (2021). Agenzia Regionale per la Prevenzione e Protezione Ambientale del Veneto. Retrieved on 21/08/2021 from https://www.arpa.veneto.it.
2. Choidis et al. (2021). A modelling approach for the assessment of climate change impact on the fungal colonization of historic timber structures. Forests, 12 (7), 819.
3. Daly (2014). The design of a legacy indicator tool for measuring climate change related impacts on built heritage. Heritage Science, 4, 19.
4. EN 15886 (2010). Conservation of cultural property - Test methods - Colour measurement of surfaces. Brussels: CEN.
5. Germinario et al. (2016). Textural and mineralogical analysis of volcanic rocks by µ-XRF mapping. Microscopy and Microanalysis, 22, 690–697.
6. Germinario et al. (2017). Trachyte weathering in the urban built environment related to air quality. Heritage Science, 5, 44.

7. Ghedini et al. (2011). Atmospheric aerosol monitoring as a strategy for the preventive conservation of urban monumental heritage: the Florence Baptistery. Atmospheric Environment, 45, 5979–5987.
8. Haugen et al. (2018). A methodology for long-term monitoring of climate change impacts on historic buildings. Geosciences, 8, 370.
9. Norsk Klimaservicesenter (2021). Norwegian Center for Climate Services. Retrieved on 22/08/2021 from https://klimaservicesenter.no.
10. Roots et al. (2011). Remote sensing of climate change, long-term monitoring of air pollution and stone material corrosion in Estonia. International Journal of Remote Sensing, 32, 9691–9705.
11. Jalón et al. (2021). Probabilistic identification of surface recession patterns in heritage buildings based on digital photogrammetry. Journal of Building Engineering 34, 101922.
12. Girardeau-Montaut D. (2016). CloudCompare, EDF R&D Telecom ParisTech.